Check for updates

Disrupted signal variability of spontaneous neural activity in children with attention-deficit/hyperactivity disorder

ZHENYAN HU,[1,4] LU LIU,[2,3,4] MENGJING WANG,[1] GAODING JIA,[1] HAIMEI LI,[2,3] FEIFEI SI,[2,3] MIN DONG,[2,3] QIUJIN QIAN,[2,3,5] AND HAIJING NIU[1,6]

[1] *State Key Laboratory of Cognitive Neuroscience and Learning & IDG/McGovern Institute for Brain Research, Beijing Normal University, Beijing 100875, China*

[2] *Peking University Sixth Hospital/Institute of Mental Health, Beijing 100191, China*

[3] *NHC Key Laboratory of Mental Health (Peking University), National Clinical Research Center for Mental Disorders (Peking University Sixth Hospital), Beijing 100191, China*

[4] *Zhenyan Hu and Lu Liu contributed equally to this research*

[5] *qianqiujin@bjmu.edu.cn*

[6] *niuhjing@bnu.edu.cn*

Abstract: Brain signal variability (BSV) has shown to be powerful in characterizing human brain development and neuropsychiatric disorders. Multiscale entropy (MSE) is a novel method for quantifying the variability of brain signal, and helps elucidate complex dynamic pathological mechanisms in children with attention-deficit/hyperactivity disorder (ADHD). Here, multiple-channel resting-state functional near-infrared spectroscopy (fNIRS) imaging data were acquired from 42 children with ADHD and 41 healthy controls (HCs) and then BSV was calculated for each participant based on the MSE analysis. Compared with HCs, ADHD group exhibited reduced BSV in both high-order and primary brain functional networks, e.g., the default mode, frontoparietal, attention and visual networks. Intriguingly, the BSV aberrations negatively correlated with ADHD symptoms in the frontoparietal network and negatively correlated with reaction time variability in the frontoparietal, default mode, somatomotor and attention networks. This study demonstrates a wide alternation in the moment-to-moment variability of spontaneous brain signal in children with ADHD, and highlights the potential for using MSE metric as a disease biomarker.

1.   Introduction

Attention-deficit/hyperactivity disorder (ADHD) is the most common neurodevelopmental disorder during childhood and adolescence, with approximately 7.2% of school-aged children meeting diagnostic criteria [1]. The children with ADHD commonly have some typical symptoms of inattention, hyperactivity and impulsivity [2], and the symptoms continue into adulthood in approximately 50% to 60% [3]. The exploration of neuropathological mechanism and development of ADHD is of significant importance.

Neuroimaging technique provides a potential tool for exploring brain function disorder in children with ADHD. Accumulating evidence has suggested dysfunction in some important brain functional connectivity and network topology in the children with ADHD. For example, Zhan et al. found the disconnection between visual and the other brain regions in children with ADHD [4]. Furthermore, it has also been found that the ADHD patients exhibited decreased global efficiency [5] and increased local efficiency [6] compared to healthy controls (HCs). These studies, from the views of large-scale network, demonstrate that brain functional organization is

disrupted in children with ADHD [5,7,8], which is also associated with the cognitive dysfunction of the disorder.

Recent progress in variability of moment-to-moment brain signal provided a new avenue for exploring local brain function using neuroimaging data. The approach of brain signal variability (BSV) has shown to be powerful in characterizing human brain development, neural function, cognitive performance and clinical conditions [9]. BSV depicts the magnitude of some aspects of variability from moment to moment in neuroimaging time series [9] and can be measured in forms of variance [10], standard deviation [11,12], mean square successive difference [13,14] or principle component analysis [15,16]. Another common approach to examine BSV is multiscale entropy (MSE, [17,18]) that quantifies signal complexity or temporal predictability in a time series [15,16]. The benefit of MSE measure is that it provides a profile of entropy across multiple time scales and assigns low values to both highly deterministic and completely random signals, which makes it explicit to measure signal complexity [16].

To quantify regularity and predictability of signals across multiple time scales, MSE requires a relatively long time series that can adequately capture the scale dependency [15]. As a novel imaging tool, functional near-infrared spectroscopy (fNIRS) is suitable for MSE analysis due to its relatively long temporal information and high sampling rate ($\geq 10Hz$) [19,20]. Furthermore, fNIRS is an ideal brain imaging tool for children with ADHD because of its natural imaging environment, portability, and tolerance for subtle head motion [19–21]. Notably, fNIRS has been previously used in exploring the neural basis underlying different cognitive demands in ADHD, such as inhibition [22], working memory [23], cognitive flexibility [24], attention [25], and emotion regulation [26]. However, since most fNIRS studies focused on the task-associated brain activation of ADHD, the investigations of intrinsic brain activity in ADHD are relatively few. Further, how the variability of brain signals was associated with the symptoms of children with ADHD remains unexplored. Recently, resting state, as an important experimental paradigm, has been introduced to fNIRS studies. The resting state is a natural imaging condition in which there is neither overt perceptual input nor behavioral output. Compared to traditional task-associated brain activation, the resting-state fNIRS (rs-fNIRS), which measures spontaneous or intrinsic neural activity in brain, can generate comparable results across different studies. Meantime, the operating procedure is relatively easy for both researchers and participants. With the resting-state fNIRS imaging, one of our previous studies has revealed that the elderly patients exhibited decreased MSE compared to HCs [27], which demonstrated the potential of fNIRS imaging technique and this MSE analysis in children with ADHD.

ADHD has been classified as a neurodevelopmental disorder in the Diagnostic and Statistical Manual of Mental Disorders fifth edition (DSM-5) [2]; what's more, both imaging and neuropsychological studies have indicated delayed maturation in ADHD [28,29]. Meanwhile, brain signal variability is widely accepted that it increases with typical development [30]. Based on the theories mentioned above, we aimed to apply MSE analyses of fNIRS data to investigate the BSV in children with ADHD. We hypothesized that children with ADHD would show decreased BSV compared with age-matched healthy children, and that such variability could be associated with ADHD symptoms and cognitive dysfunction.

2. Materials and methods

2.1. Participants

Forty-two boys with ADHD (aged 8 to 12 years old, Mean ± SD = 9.4 ± 1.1) were recruited from the clinics of Peking University Sixth Hospital/Institute of Mental Health. The diagnosis of ADHD was determined by an experienced psychiatrist using the Clinical Diagnostic Interview Scale (CDIS) [31,32] in a semi-structured interview according to the criteria of the Diagnostic and Statistical Manual of Mental Disorders, Fourth Edition. The inclusion criteria were as follows: 1) right-handedness; 2) full scale estimated IQ using the Chinese Wechsler Intelligence

Scale for Children [33] ≥ 80; 3) medication-naïve (stimulant and non- stimulant medications) and free of other medical interventions. Patients with a diagnosis of schizophrenia, pervasive developmental disorders, bipolar disorder, epilepsy, mental retardation, or other brain disorders were excluded. It should be noted that this study only focused on boys with ADHD considering that ADHD is more frequently prominent in males with a male-to-female ratio of 4:1 in clinical samples [34].

Forty-one age-matched healthy control boys (aged 8 to 11 years old, Mean ± SD = 9.5 ± 0.8) were enrolled from a primary school in the local community. Individuals with ADHD, mania, bipolar disorder, other major psychiatric disorders, family history of psychosis, and severe physical diseases were excluded.

This study was approved by the Medical Research Ethics Committee of Peking University Sixth Hospital. Written informed consent was obtained from the parents of all participants (and participants themselves if they were at least 10 years old) before the experiment.

2.2. Diagnoses and assessment

In addition to the clarification of an ADHD diagnosis, the CDIS was also used to assess ADHD subtypes and evaluate comorbidities. Among the recruited boys with ADHD, 22 (52.4%) met the criteria for the predominantly inattentive subtype (ADHD-I), and 20 (47.6%) met the criteria for the combined subtype (ADHD-C) (Table 1). Regarding comorbidities, 8 (19.0%) had disruptive behavior disorder (DBD), including 7 (16.7%) with oppositional defiant disorder (ODD) and 1 (2.4%) with DBD-not otherwise specified (DBD-NOS); 1 (2.4%) had social phobia, 1 (2.4%) had major depression disorder, 8 (19.0%) had a tic disorder, and 19 (45.2%) had a learning disorder.

Table 1. Demographic and clinical characteristics of ADHD and HCs

Characteristics	ADHD (n=42)	HCs (n=41)	*T value*	*P* value
Age in years (Mean ± SD)	9.4 ± 1.1	9.5 ± 0.8	-0.23	0.819 [a]
IQ (Mean ± SD)	110.3 ± 13.5	115.3 ± 11.6	-1.80	0.076 [a]
ADHD subtype (n, %)				
ADHD-I	22 (52.4)	—	—	—
ADHD-C	20 (47.6)	—	—	—
ADHD symptoms (Mean ± SD)				
Inattentive	17.8 ± 3.2	8.8 ± 4.7	10.32	<0.001 [a]
Hyperactive/Impulsive	12.7 ± 6.0	7.3 ± 4.5	4.66	<0.001 [a]
Total	30.6 ± 7.8	16.1 ± 8.5	8.09	<0.001 [a]

Abbreviations: ADHD, attention-deficit/hyperactivity disorder; HCs, healthy controls; SD, standard deviation; IQ, intelligence quotient; ADHD-I, ADHD inattentive subtype; ADHD-C, ADHD combined subtype.
[a]The *P* value was obtained using two-sample t-test.

The cognitive function was assessed using the reaction time variability (RTV) index adopted from a Stop Signal Task in the Cambridge Neuropsychological Test Automated Battery (CANTAB). Each participant was asked to complete a 20-min task, in which the participant must respond to an arrow stimulus by selecting one of two options, depending on the direction at which the arrow points. The RTV was calculated as the ratio of standard deviation to mean value of the reaction time for correct responses for analyses [35]. The RTV data were only available for 39 ADHD patients (21 ADHD-I and 18 ADHD-C) and 24 HCs.

2.3. Data acquisition

A multichannel near-infrared optical imaging system (Hui Chuang, China) with continuous waves and a 17 Hz sampling rate was used to collect rs-fNIRS data. Similar to our previous study

[5], twenty-four light sources (each with two wavelengths: 670 and 830 nm) and twenty-eight detectors were arranged on the participant's head, with adjacent source and detector pairs being 3 cm apart and composed of 80 different measurement channels (Fig. 1(A)). Using the external auditory canals and vertex of the participants as landmarks, the position of these probes was established according to the international 10-20 system. Specifically, measurement channels 35 and 36 were placed around T3 and T4, and the midpoint of the two channels was localized in Cz (Fig. 1(B)). Considering changes of the averaged head circumference from 51.5 cm in 8-years-old children to 53.2 cm in 12-years-old children [36], we estimated the measurement inconsistency across participants was in the range of 0.09 cm (i.e., [(53.2-51.5)/53.2] × 3 cm; 3cm is the S-D separation). The positions of the measurement channels were validated by the spatial coordinates, which were acquired from the structural MRI image of an arbitrary participant with a Siemens 3.0 Tesla scanner. The channels were labeled with vitamin E capsules during structural MRI scanning and were projected on the network templates from Yeo et al. [37] in further analyses. According to the templates, six functional networks, i.e., default mode (DMN), frontoparietal (FPN), ventral attention (VAN), somatomotor (SMN), dorsal attention (DAN) and visual (VN) networks, were involved and displayed with different colors in our study (Fig. 1(C)).
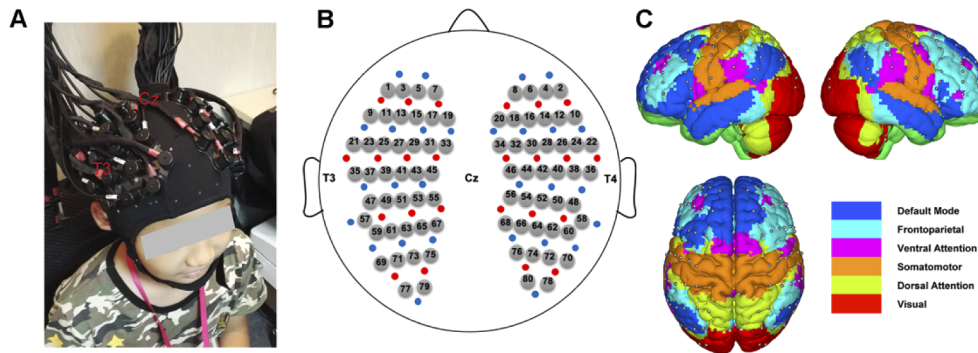

Fig. 1. Schematic illustration of experimental data collection. (A) Photograph of fNIRS data collection from a participant. (B-C) The arrangement of the whole-head 80 measurement channels on a structural brain template, the red and blue dots represent the sources and detectors, respectively. (B) and a functional network template (C) [37].

2.4. Data preprocessing

The in-house FC-NIRS package (http://www.nitrc.org/projects/fcnirs [19]) was used to preprocess the current resting-state fNIRS data in this study. First, motion artifacts were examined and removed from the optical signals using a spline interpolation method [38]. This method detected the motion-induced artifacts by calculating moving standard deviation (MSD) within sliding time windows in a window length of 2 seconds. The MSD values larger than a predefined threshold (e.g., 5 MSD [19]) were regarded as artifacts. The time series that represented the motion artifacts was further modeled via a cubic spline interpolation, which was then subtracted from the original signal of the time series. The resulting signal was considered to be free of motion artifacts. Next, the signals were bandpass filtered with a frequency of 0.01 Hz-0.1 Hz [39] to diminish the interference of low-frequency drift and high-frequency neurophysiological noise [40]. Subsequently, they were transformed into the concentrations of oxyhemoglobin (HbO) and deoxyhemoglobin (HbR) using the modified Beer-Lambert law [41] with a differential path-length factor of 6 for two wavelengths [41–45]. Finally, an eight-minute stable hemoglobin time series was extracted from each participant. Note that the HbO data were used for subsequent analysis considering its better signal-to-noise ratio [46].

2.5. Multiscale entropy and brain signal variability

The multiscale entropy (MSE) algorithm, which has been widely used for characterizing neural signal complexity, was adopted to estimate brain signal variability (BSV) in this study. MSE was calculated according to the following steps similar to our previous research [27]. First, the HbO concentration time series $\{x_1, \ldots x_i, \ldots x_N\}$ was downsampled to obtain a coarse-grained time series for different timescales t. The coarse-grained time series y^t was generated by averaging the data points within nonoverlapping windows of length t. Each value of the coarse-grained time series, y_j^t, was computed using the following equation:

$$y_j^t = \frac{1}{t} \sum_{i=(j-1)t+1}^{jt} x_i, \ 1 \le j \le \frac{N}{t} \ . \tag{1}$$

x_i denotes the value of time point i in the original time series; N defines the number of time points; and j is the index of each coarse-grained time series. Second, the sample entropy of each downsampled time series, S_E, was calculated by:

$$S_E(m, r) = - \ln \frac{C_{m+1}(r)}{C_m(r)}, \tag{2}$$

where

$$C_m(r) = \frac{number\ of\ pairs(i, j)\ with\ |v_i^m - v_j^m| < r \times STD(y)}{number\ of\ all\ probable\ pairs}. \tag{3}$$

In Eqs. (2) and (3), m defines the pattern length indicating that m consecutive data points are used for pattern matching, and r specifies the similarity criterion indicating the threshold portion of the time series standard. In this study, pattern length was set to $m=2$ and the similarity criterion was chosen to $r=0.2$, which were judged to be optimal and statistically valid following the method used in [27,47,48]. The data points are considered to have indistinguishable amplitude values when the absolute amplitude difference among them is lower than r. v_i^m is the vector defined as $\{v_i^m = y_i, y_{i+1}, \ldots y_{i+m-1}\}$; the definition of v_j^m is similar to that of v_i^m, and $|v_i^m - v_j^m|$ means the Chebychev distance between v_i^m and v_j^m.

MSE, the sample entropy across different temporal scales, quantifies the signal variability by estimating the predictability of amplitude patterns across a time series. While lower MSE values indicate a low complexity and a high degree of determinacy for the signal, higher MSE values reflect a high complexity and a low degree of predictability or rich information for the signal.

2.6. Statistical analysis

2.6.1. Between-group differences in brain signal variability

To evaluate group differences in BSV, the MSE values of each channel between the ADHD and HCs were compared using a multiple linear regression model, in which MSE was considered as dependent variable, group as independent variable, and age, IQ, age × group (i.e., interaction effect of age and group) and IQ × group as covariates. In the model, significant group differences were determined by P values lower than 0.05. False discovery rate (FDR) correction [49] was used to control the multiple testing error by correcting P values.

2.6.2. Correlation between brain signal variability and ADHD core symptoms/reaction time variability

Pearson correlation analyses were performed between MSE and ADHD symptom scores (inattentive, hyperactive/impulsive and total scores) as well as between MSE and RTV in the ADHD and HCs, respectively. Before the correlation analyses, the effects of age and IQ were removed by multiple linear regression. FDR correction was conducted to correct the multiple comparisons.

3. Results

3.1. *Demographic and core symptom*

The demographic and core symptom data are presented in Table 1. There were no significant differences in age ($P = 0.819$) or IQ ($P = 0.076$) between the ADHD and HCs. The ADHD group had significantly higher inattentive scores ($P < 0.001$), hyperactive/impulsive scores ($P < 0.001$) and total scores ($P < 0.001$) than the HCs group.

3.2. *Spatial distribution of brain signal variability in the ADHD and HCs*

Similar to previous studies [27,47,50], the area under the curve (AUC) according to the sample entropy across different temporal scales (i.e., MSE) was adopted to evaluate brain signal variability (BSV). To obtain an intuitive visual presentation, we adopted bilinear interpolation algorithm to smooth MSE values across the whole brain. The bilinear interpolation algorithm performs interpolation calculations in both directions and can be extended from the linear interpolation between variables. Figure 2(A) shows the group-averaged MSE in ADHD and HC groups,
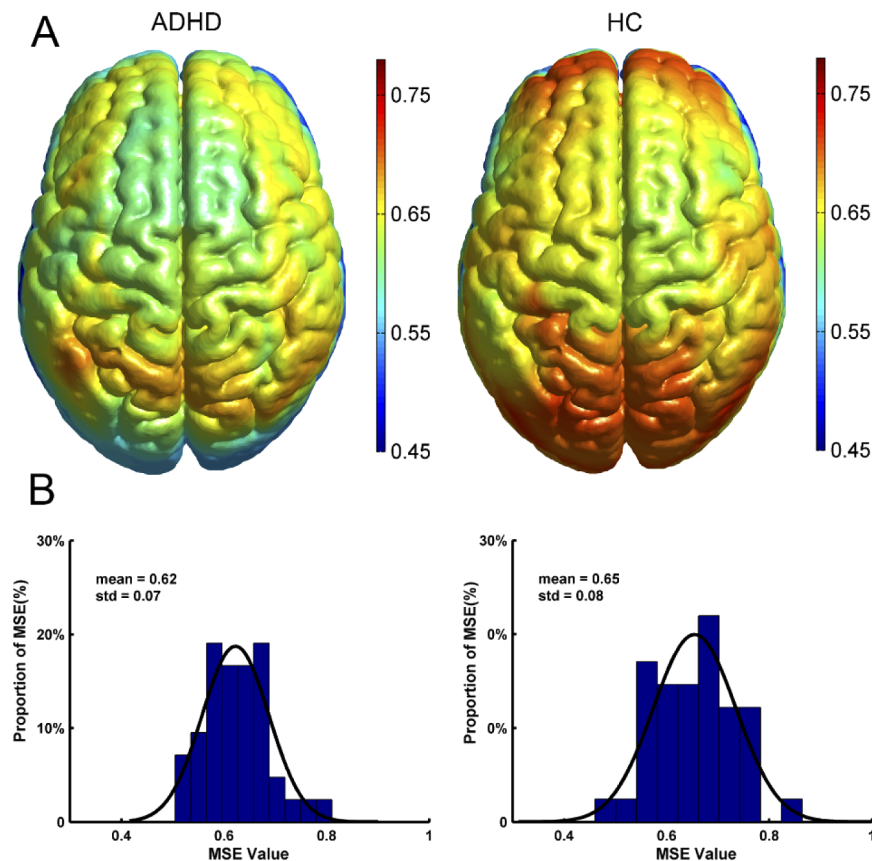

Fig. 2. MSE and its distribution. (A) The spatial maps of MSE in the whole brain for the ADHD and HC groups, which were smoothed with bilinear interpolation algorithm and implemented in MATLAB. The red color indicating higher MSE values and the blue color indicating lower MSE values. (B) Histogram distribution of MSE values among participants. The MSE distributions of both the ADHD and HC groups display approximately normal configurations.